Available online at BCREC website: https://bcrec.id

Bulletin of Chemical Reaction Engineering & Catalysis, 15 (3) 2020, 662-673

Research Article

Natural Clay of Pasaman Barat Enriched by CaO of Chicken Eggshells as Catalyst for Biodiesel Production

S. Syukri*, Kevin Septioga, Syukri Arief, Yulia Eka Putri, Mai Efdi, Upita Septiani

Department of Chemistry, Andalas University, Jl. Universitas Andalas, Limau Manis, Padang 25163, Indonesia.

Received: 9th June 2020; Revised: 10th August 2020; Accepted: 11th August 2020; Available online: 14th September 2020; Published regularly: December 2020

Abstract

This study uses broiler chicken eggshells to enhance catalytic activity of clay obtained from Pasaman Barat (West Sumatra, Indonesia) in lab-scale biodiesel production. The eggshell is a source of calcium oxide (CaO) which operates as a catalyst when mixed with the clay (Ca-Clay). Two other catalysts were also prepared as comparisons by 1) heating the clay at 800 ^{o}C for 6 hours (P-Clay), 2) mixing the P-Clay with KOH (K-Clay). An X-ray Fluorescence (XRF) showed the elemental composition of Ca-Clay contained Ca, Si, Al, and Fe. An X-ray Diffraction (XRD) showed the formation of highly crystalline CaO in the Ca-Clay with the main peak at 2θ = 37.27^{o}. The Fourier Transform Infra Red (FTIR) spectrum showed an absorption peak in the range of 700-900 cm^{-1} indicating Ca-O stretching demonstrating successful incorporation of the CaO into the clay. The catalytic activity test showed the Ca-Clay had a higher catalytic performance than P-Clay and K-Clay in terms of the yield of biodiesel produced (73%).

Keywords: Eggshell; Natural Clay; Heterogeneous catalyst; Biodiesel; natural

How to Cite: Syukri, S., Septioga, K., Arief, S., Putri, Y.E., Efdi, M., Septiani, U. (2020). Natural Clay of Pasaman Barat Enriched by CaO of Chicken Eggshells as Catalyst for Biodiesel Production. *Bulletin of Chemical Reaction Engineering & Catalysis*, 15(3), 662-673 (doi:10.9767/bcrec.15.3.8097.662-673)

Permalink/DOI: https://doi.org/10.9767/bcrec.15.3.8097.662-673

1. Introduction

In recent times, diesel engines have been a subject of much research focusing on reducing emissions and improving their economy. Petroleum-based middle-distillate fuel has many disadvantages so alternative and renewable fuels are being developed. Proposals for practical environmentally friendly fuel production abound using the non-fossil fuel sources ethanol and vegetable oil. It has been shown that vegetable oil is a promising alternative fuel for a diesel engine. However, the use of unrefined vegetable oil may cause trouble in a diesel engine because of its high viscosity and low volatility. This problem can be solved through transesterification with short-chain alcohols to produce fatty acid methyl ester, which is known as FAME or biodiesel [1].

Biodiesel has similar qualities and characteristics to fossil diesel but burns more cleanly. Several years of commercial use have proven that it can be used successfully in diesel engines. Biodiesel can be obtained from renewable, sustainable resources and also has lower greenhouse gas emissions compared to fossil diesel

* Corresponding Author.
E-mail: syukri.darajat@yahoo.com
syukridarajat@sci.unand.ac.id (S. Syukri);
Telp: +62-751-71161

[3]. A comparison between the physicochemical properties of diesel and biodiesel is presented in Table 1. Transesterification is a chemical reaction between triglycerides and short-chain alcohols in the presence of a catalyst to produce mono-esters as shown in Figure 1. When methanol is used in transesterification, it is termed methanolysis. In transesterification, triglyceride is converted into mono-esters and glycerol while the esterification reaction uses free fatty acids and methanol [2].

One of the most important variables affecting the yield of esters is the molar ratio of alcohol to triglycerides. The stoichiometric ratio for transesterification requires three moles of alcohol and one mole of triglycerides to produce three moles of fatty acid alkyl esters and one mole of glycerol. Because the transesterification reaction is reversible, large amounts of alcohol are necessary to shift the reaction to the right. For maximum conversion to esters, a 6:1 molar ratio is used. The molar ratio does not affect acid, peroxide, saponification, and iodine methyl ester values. However, the high molar ratio of alcohol to vegetable oils disrupts glycerol separation because there is an increase in solubility. When glycerol remains in solution, it helps shift the balance back to the left, then decreasing the yield of ester [4]. Transesterification decreases the viscosity of the vegetable oils to a value that can be handled by diesel engines by reducing the length of the molecular chains by 1/3. The Cetane number or combustion speed is consequently increased enhancing the heating value [5].

Three kinds of catalysts are commonly used in biodiesel production to speed the reaction toward equilibrium; conventional bases, acids, and more recently enzymes. Acidic and basic catalysts can be categorized as homogeneous or heterogeneous catalysts [6]. Acid-based catalysts, such as: H_2SO_4 and HCL, and basic catalysts, such as: KOH and NaOH, are all homogeneous and are used in current commercial biodiesel production. Acid-based homogeneous catalysts operate at high temperatures, are difficult to recycle, corrosive, and also require considerable time to reach equilibrium during biodiesel production. Base-based homogeneous catalysts have high catalytic performance and

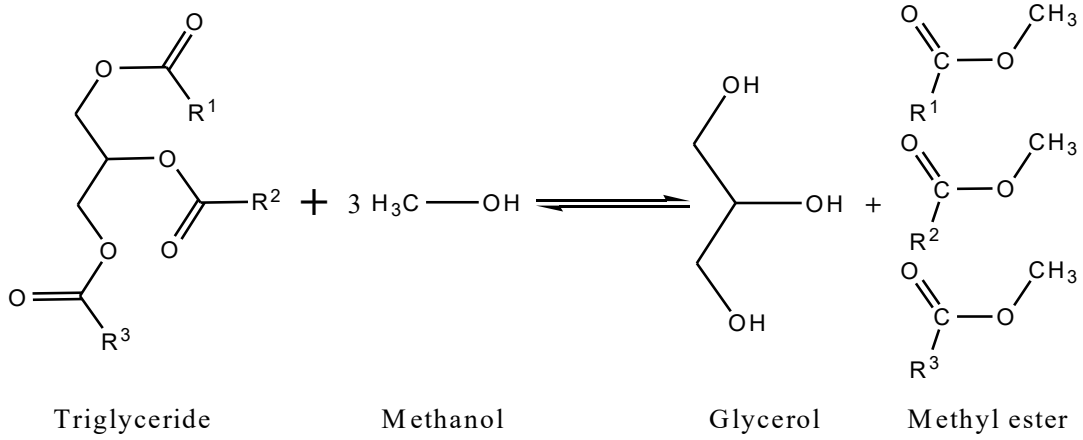

Figure 1. Mechanism of the transesterification reaction.

Table 1. Specification of diesel and biodiesel fuel [39]

Fuel Properties	Diesel	Biodiesel
Fuel standard	ASTM D975	ASTM PS 121
Fuel composition	C_{10} – C_{21} HC	C_{12}-C_{22} FAME
Kinematic viscosity @40°C (mm^2/s)	1.3–4.1	1.9–6.0
Density @15°C (kg/m^3)	848	878
Water (ppm by wt.)	161	0.05% max
Sulfur (wt.%)	0.05 max	0–0.0024
Boiling point (°C)	188–343	182–338
Flash point (°C)	60–80	100–170
Cetane number	40–55	48–65

result in high-quality product but separating the base catalyst from product and waste is expensive and not environmentally friendly. Moreover, a homogeneous base catalyst needs high-quality vegetable oil to prevent side reactions like saponification and hydrolysis.

The problems with these homogenous catalysts are a motivation to develop heterogeneous catalysts, which can be more effective and environmentally friendly. A heterogeneous catalyst can reduce production costs and also enhance sustainability. Since the catalyst is in a different phase than the reactant/product, usually a solid, product separation and the catalyst recovery is quite easy. Depending on the form of the catalyst used, and the preparation method, heterogeneous catalysts require high transesterification pressure and temperature for high yields. Also, the physical and structural properties of catalysts need to be adequately formulated during preparation to maximize results [3]. Compounds used in heterogeneous base catalysts that have been developed to synthesize biodiesel include alkaline earth metal oxides, zeolite, hydrotalcite, and mixed transition metal oxides [7]. Synthesis of catalysts using silica hybrids with transition metals, such as: silica-Co [8] and Silica-Mn [9], have been tested.

Clay minerals have diverse applications based on clay's unique surface properties. The porous heterostructure of clay minerals lends it to industry application based on its catalytic performance and absorption [10]. In biodiesel production, clay functions as a molecular sieve that is used to facilitate the reactions of esterification or transesterification, while also facilitating the recyclability of the catalyst [11]. The properties of this material mainly depend on the structure and composition of certain clay minerals. For example, specific surface area and other surface properties of clay minerals control the catalytic process [12]. In addition, clay does not interfere with the quality of biodiesel, it is a natural resource and produces no industrial waste [13]. CaO on its own can catalyze the transesterification reaction but is not stable in the reaction medium [14]. However, $CaO\text{-}SiO_2$ has been used successfully as a catalyst in the reaction of producing biodiesel [15]. Chicken eggshells, being rich in Ca could potentially be used to produce CaO to support a clay catalyst which is also SiO_2 rich.

The present work aims to determine the characteristics of broiler chicken eggshell waste and natural clay samples from Pasaman Barat regency, to characterize a material made from CaO from eggshell waste mixed with natural clay and determine its catalytic activity in the transesterification reaction of vegetable oil to make biodiesel.

2. Materials and Methods

2.1 Materials

Natural clay was collected from Pasaman Barat regency, Sumatra Barat Province. The broiler chicken eggshell was collected from Andalas University cafeteria. The vegetable oil used for the transesterification study was processed palm oil purchased from the local market. Potassium hydroxide (KOH) (Merck), methanol (Analysis Grade) (Merck) and NaOH (Merck) were also used.

2.2 Catalyst Preparation

2.2.1 Eggshell

The eggshell was rinsed with water, and the membrane and surface dirt removed. Then it was rinsed again with distilled water. Eggshells were then dried using an oven (110 ^oC for 1 hour), crushed by mortar and pestle then passed with a 90 µm sieve. After that, the sample was calcined at 800 ^oC for 10 hours [16]. The sample before and after calcination was characterized by XRF and XRD.

2.2.2 Clay

Clay was heated at 110 ^oC for 2 hours, crushed and sifted to 180 µm. In this study, the original clay was named O-Clay. The O-Clay was washed in distilled water, then centrifuged. The solids were separated and dried at 110 ^oC for 3 hours, then crushed and sifted. The clay powder was heated again at 150 ^oC for 3 hours and cooled [17]. 35 g of O-Clay was calcined at 800 ^oC for 10 hours [2], then crushed and sifted at size 180 µm. This sample was named parent clay (P-Clay), which was then characterized by XRD, XRF, and FTIR.

2.2.3 Ca-Clay

20 g of P-Clay was weighed and mixed with 0.4 M NaOH in a 250 mL glass beaker. The mixture was stirred and heated at 65 ^oC for 6 hours. The precipitate was separated by filtration with Whatman 41 filter paper and rinsed with distilled water several times. The precipitate was dried at 110 ^oC for 3 hours, then crushed and passed through a 180 µm sieve. The sample was calcined at 500 ^oC for 6 hours and labeled Activated-Clay. The composition

was prepared by mixing 10 g of Activated-Clay and 8.24 g of CaO (1 g Activated-Clay: 15 mmol CaO) in 100 mL of water. The mixture was washed with 100 mL distilled water and stirred for 24 hours at 65 °C. The mixture was filtered with filter paper, then heated to remove water at around 110 °C. The mixture was calcined at 800 °C for 6 hours [2]. The final mixture was labeled Ca-Clay and characterized by XRF, XRD, and FTIR.

2.2.4 Reference catalyst (K-Clay)

15 g of P-Clay was weighed and dissolved in a 0.5 M 150 mL KOH solution (with a ratio of clay: KOH = 1:10 m/v), stirred with a magnetic stirrer for 24 hours at 65 °C. The precipitate was separated by filtration with Whatman 41 filter paper and rinsed with distilled water several times. The precipitate was dried at 110 °C for 3 hours, then crushed and passed through a 180 µm sieve to obtain the maximum specific surface area. The sample was calcined at 500 °C for 6 hours [17]. The samples were labeled K-Clay and then characterized by XRF, XRD, and FTIR.

2.2.5 Characterization of catalyst

The physicochemical properties of the synthesized catalysts were studied by X-ray Fluorescence (XRF) (NEXCG Rigaku), X-ray Diffraction (XRD) (X'Port PAN Analytic), Fourier Transform Infra-Red (FTIR) (Thermo Scientific: Nicolet iS10).

2.2.6 Reaction procedure

Commercial palm oil with a free fatty acid level of 0.4527% [17] was used. Transesterification of this oil (which contains triglycerides) into biodiesel (methyl ester) was carried out in a 250 mL three-necked flask connected to condenser for the reflux process equipped with a temperature indicator on top of a magnetic stirrer hotplate. The molar ratio of palm oil and methanol used in this study was 1:6, and the amount of catalyst used 1%, 3%, or 5% of the weight of palm oil. At first, the catalyst and methanol were heated to 50 °C with continuous stirring. 108 mL of palm oil was added to the three-neck flask, which had been heated to 110 °C until there were no more bubbles from the water content the temperature was allowed to drop to 50 °C. The catalyst, methanol, and palm oil were then mixed. The transesterification reaction was carried out for 4 hours at 60 °C with continuous stirring. At the end of the reaction, the flask was cooled to room temperature, and the catalyst was separated from the mixture using filter paper. Biodiesel products were separated from glycerol using a separating funnel. Biodiesel was washed with hot distilled water (50 °C) with a volume ratio of 1:1 and shaken for 5 minutes forming a white liquid. The mixture was allowed to settle and the water was collected at the bottom. Biodiesel was heated at a temperature above the boiling point of water (110 °C) until there were no more water bubbles [17]. The main chemical components contained in the product were analyzed using GC-MS and Viscosity (ASTM D-445-10). The content of FAME in the biodiesel produced was analyzed by GC using a DBwax capillary column (Agilent JW Scientific) and Flame Ionization Detector (FID) as in Suryaputra [18] The injector temperature was 250 °C at splitless condition and FID was set at 300 °C. Yield was calculated in Equation (1).

$$Yield(\%) = \frac{Mass\ of\ Biodiesel \times \%FAME\ in\ sample}{Mass\ of\ Palm\ Oil} \times 100\% \quad (1)$$

3. Results and Discussions

3.1 Broiler Chicken Eggshell Waste

Based on the XRF analysis of eggshell, the amount of calcium found in broiler chicken eggshell waste was 70% and did not show a significant change after calcination. The other elements found in broiler chicken shells included Mg, Al, Zr, Si, S, Zn, and K. The main composition of the eggshell was $CaCO_3$, which decomposed to CaO during calcination. This transformation was proved by the changes in the XRD pattern as shown in Figure 2. After calcination at 800 °C, the color of eggshell powder became bright white (Figure 3) which is typical of CaO [19].

The XRD patterns in Figure 2 showed the pure broiler chicken eggshell powder before and after calcination. The patterns showed that the samples have a high crystallinity compared with the standard data of $CaCO_3$ (ICSD 158258) and CaO (ICSD 51409). The $CaCO_3$ has a main peak at $2\theta = 29.33^o$ and supporting peaks are at $2\theta = 22.99^o$; 35.93^o; 39.37^o, and 47.47^o. On the other hand, CaO has a main peak at $2\theta = 37.27^o$. The presence of several additional peaks showed the presence of $Ca(OH)_2$ in the calcined sample due to the reaction between CaO and H_2O in the air, however, the presence of $Ca(OH)_2$ was negligible.

3.2. pH Analysis of Clay

The calcination at 800 °C was intended to remove the organic compounds from the clay, and this treatment changed the color of the clay to red (P-Clay). The increase in pH of P-Clay (Table 2) indicated that the organic compounds have been dissipated releasing H^+ ions from the clay. Theoretically, some organic compounds can detach from clay starting from 100 °C [20].

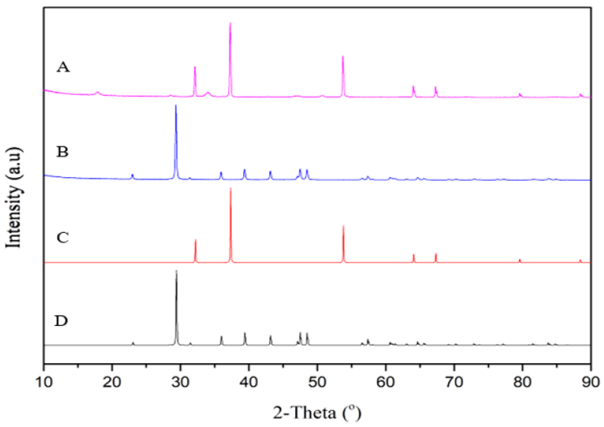

Figure 2. Diffractogram of (A) pure broiler chicken eggshells and (B) after calcined at 800 °C compared with the standard data (C) CaO and (D) $CaCO_3$.

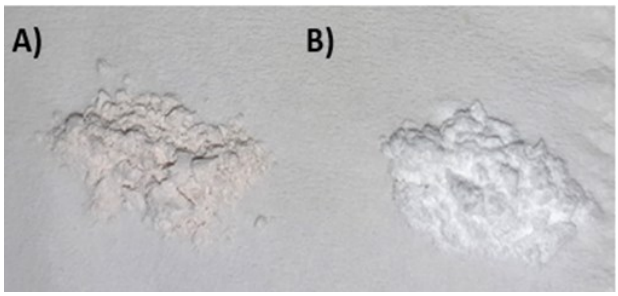

Figure 3. Eggshell powder (a) before calcined and (b) after calcined at 800 °C.

P-Clay was mixed with KOH to increase its catalytically active surface. This resulted in an increase in sites facilitating the occurrence of cation exchange as evidenced in the clay XRF data (Figure 4), and by the increase of pH value during the impregnation of K^+ ions. XRF measurements showed an increase in potassium levels indicating that the cation was successfully embedded in P-Clay. In the interlayer of the P-Clay K^+ ions replaced the remaining H^+ ions. Modification of clay with CaO increased its pH value to 12.324, because CaO reacts readily with air to form $Ca(OH)_2$, which is a strong base.

3.3 XRF Analysis of Clay Catalyst

Based on XRF data (Figure 4), composition of clay in Pasaman Barat is dominated by iron (66.9%), silicon (20.5%), and aluminum (7.85%). The other elements found in clay samples were titanium, magnesium, calcium, potassium, sodium. After calcination, this composition changed, iron content decreased to 51.9%, while silicon and aluminum increased to 31.5% and 10.4%. The KOH impregnation process in the P-Clay sample was evidenced by the XRF analysis results which showed an in-

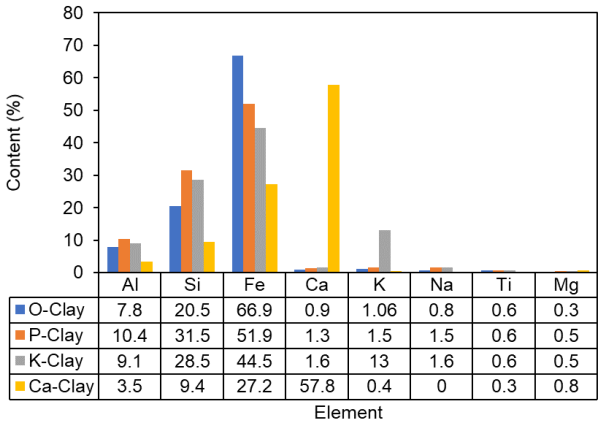

	Al	Si	Fe	Ca	K	Na	Ti	Mg
O-Clay	7.8	20.5	66.9	0.9	1.06	0.8	0.6	0.3
P-Clay	10.4	31.5	51.9	1.3	1.5	1.5	0.6	0.5
K-Clay	9.1	28.5	44.5	1.6	13	1.6	0.6	0.5
Ca-Clay	3.5	9.4	27.2	57.8	0.4	0	0.3	0.8

Figure 4. XRF data of clay composition.

Table 2. Characteristics of natural clay and modified clay.

Characteristic	O-Clay	P-Clay	K-Clay	Ca-Clay
Color				
pH	4.948	6.712	9.712	12.324

crease in potassium from 1.5% to 13.0%. Meanwhile, mixing P-Clay with CaO increased in calcium from 1.3% to 57.8%. The solubility in water and the atomic radius were the main factors that result in the low levels of potassium elements in K-Clay compared to calcium in Ca-Clay. K_2O is more soluble in water compared to CaO, and this causes some impregnated potassium in the clay to detach. Moreover, the size of a potassium atom is relatively larger than calcium, thus it is more difficult for potassium to enter the pores in the clay particles.

3.4 FTIR Analysis of Clay Catalyst

Infrared spectroscopy was carried out to assess the chemical changes in the clay samples by identifying the presence of inorganic functional groups in the clay structure through absorption bands of the FTIR spectrum. This spectrum shows peaks corresponding to the typical vibrations of the functional groups present. Two regions of the spectrum where examined; the fingerprint area with a frequency of 400-1300 cm^{-1} and functional group area with a frequency of 1300-4000 cm^{-1} [21]. The stretching O-H vibrations in silicate layers appear in the 3400-3750 cm^{-1} region. Bending H-O-H vibration occurs in the area between 600-950 cm^{-1}. Si-O and Al-O are stretching in the tetrahedral and octahedral layers found in the range between 700-1200 cm^{-1}. Bending vibration for Si-O-Si and Al-O-Al bonds is predominantly found in the area between 150-600 cm^{-1}, while interlayer vibration is found in the region between 50-150 cm^{-1} [22]. The spectra obtained in this study are in the range of 600-4000 cm^{-1} region.

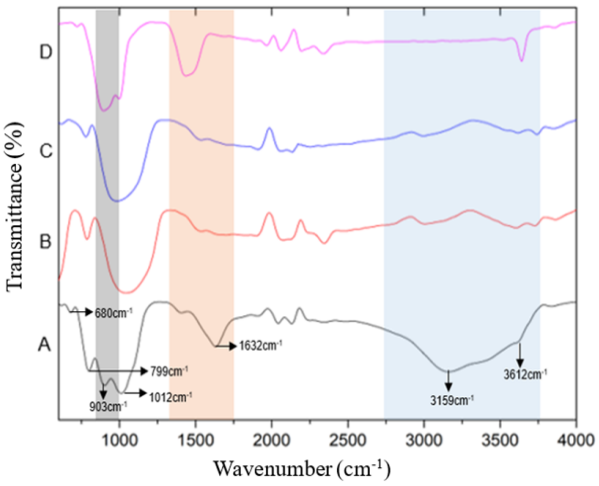

Figure 5. Spectra FTIR (A) O-Clay, (B) P-Clay, (C) K-Clay dan (D) Ca-Clay.

Figure 5A shows the absorption bands of O-Clay. Characteristics of the OH group appears on absorption bands around 3700-3400 cm^{-1} [23] and hydroxyl stretching vibration at 3612 cm^{-1}. The OH groups are located between octahedral and tetrahedral sheets in the clay interlayer, so OH groups form weak hydrogen bonds to the Si-O-Si bond [24]. The absorption band at 3450-3100 cm^{-1} is associated with O-H stretching vibration of H_2O-H_2O, because the O-Clay contains absorbed water [25,26]. The absorption band, 1900-2624 cm^{-1} is related to the OH vibration of the hydroxyl molecule presented in all-natural hydrate silicates [27]. The wavenumber at 1632 cm^{-1} is a bending vibration of H-O-H because of the vibration deformation in the absorbed H_2O group [28]. Si-O stretching vibration in the tetrahedral layer is indicated by a sharp absorption band at 1012 cm^{-1}, which is characteristic of SiO_2 [29]. Bending vibration from the core hydroxyl is shown in the absorption band 903 cm^{-1} which is a result of the bond between a proton and coordinated oxygen from Al^{3+} on an octahedral side which produces vibration deformation from Al-OH-Al and also shows the presence of montmorillonite crystals in the sample. In the natural clay spectra, Si-O vibrations at wavenumber 799 cm^{-1} indicate the presence of quartz minerals in the clays. The bending vibration of Si-O-Al is at a wavenumber 680 cm^{-1} [27,28,30].

Figure 5 showed the changes in the pattern of absorption bands after each addition. The change in absorption patterns in the range of 2750-3750 cm^{-1} can be attributed to O-H vibrations, indicating the release of water molecules during the heating process [20]. This fact is also supported by the loss of the 900-1000 cm^{-1} absorption band, which is a bending vibration of Al-O-H. This absorption band is replaced by a new band at 786 cm^{-1}, which is typical for octahedral coordination Al^{3+}, which changes to tetrahedral coordination [31,32].

Figure 5D, showed the clay's ability to absorb CO_2, as evidenced by the quite sharp absorption band 1300-1500 cm^{-1}, which is stretching C-O vibration of absorbed CO_2 [16]. The presence of $Ca(OH)_2$ is indicated by the emergence of stretching absorption bands from O-H at 3641 cm^{-1} and also the Ca-O stretching in 700-900 cm^{-1} absorption band [18,33] that is supported by XRD data in Figure 6. These results indicate that neither CaO or KOH addition significantly alter the FTIR pattern of P-Clay.

$$2\ FeOOH.nH_2O \rightarrow Fe_2O_3 + (n+1)H_2O \quad (2)$$

3.5 XRD Analysis of Clay Catalyst

Clay naturally contains minerals such as kaolinite, illite, smectite, quartz. The types of minerals in a clay can be identified with XRD based on the position of two theta according to the ICSD standard. XRD showed that the samples contained goethite, quartz, illite, montmorillonite, and muscovite as shown in Figure 6. Goethite was found to be the main component with 66.9% iron content, and this value concurs with XRF data (Figure 4). The high peak intensity of the XRD pattern at 2θ = 26.5° showed that natural clay has high crystallinity. However, additional intensity peaks near this angle were due to the presence of minerals quartz, montmorillonite, muscovite, and illite. When the clay was heated at 800 °C, the goethite changes into hematite based on the reaction (2) [34]:

The impregnation of K^+ from KOH did not alter the basic XRD pattern of P-Clay (Figure 6b) but slightly reduced the intensity of hematite peaks (2θ = 24.12°; 33.12°; 35.6°; 40.88°) and montmorillonite peaks (2θ = 13.83°; 19.65°). The decrease in intensity may occur due to the substitution of Fe^{3+} cations with K^+, and then this has an impact on the structure of hematite mineral crystals, which is supported by XRF data. Figure 6d showed several peaks with low intensity at 2θ = 32.17°; 37.33°, 53.81°, and 64.09° corresponding to CaO. In addition, $Ca(OH)_2$ peaks at 2θ = 18.09°; 28.79°; 34.19°; 47.23°; 50.95° have high intensity as the CaO reacts quickly with water vapor in the atmosphere forming $Ca(OH)_2$ as is also demonstrated in the FTIR spectra in Figure 6 [35].

3.6 Transesterification Reaction

3.6.1 Catalytic activity

The catalytic activity test was only carried out for P-Clay, K-Clay, and Ca-Clay (Figure 7). All three types of modified clay demonstrated catalytic activity Concentration of 1%, 3%, and 5% were tested. In a transesterification catalyst reaction, clay has a role in forming the methoxide anions, which bind to triglycerides, then convert triglycerides to diglycerides, and diglycerides are then converted into monoglycerides.

In general, Ca-Clay showed higher catalytic activity than P-Clay and K-Clay. Ca-Clay's excellent catalytic activity is due to the oxygen on the surface binding with H^+ from methanol which results in OH^- formation. There was a high concentration of Ca in Ca-Clay (57.8 %), so the surface contained a large amount of CaO. The low catalytic activity of K-Clay is due to the high concentration of embedded K (Figure 4) which means it has a high tendency to form Al-O-K from KOH and Al-O-H during the calcination process. The formation of Al-O-K reduces its catalytic activity and lowered biodiesel yield [36].

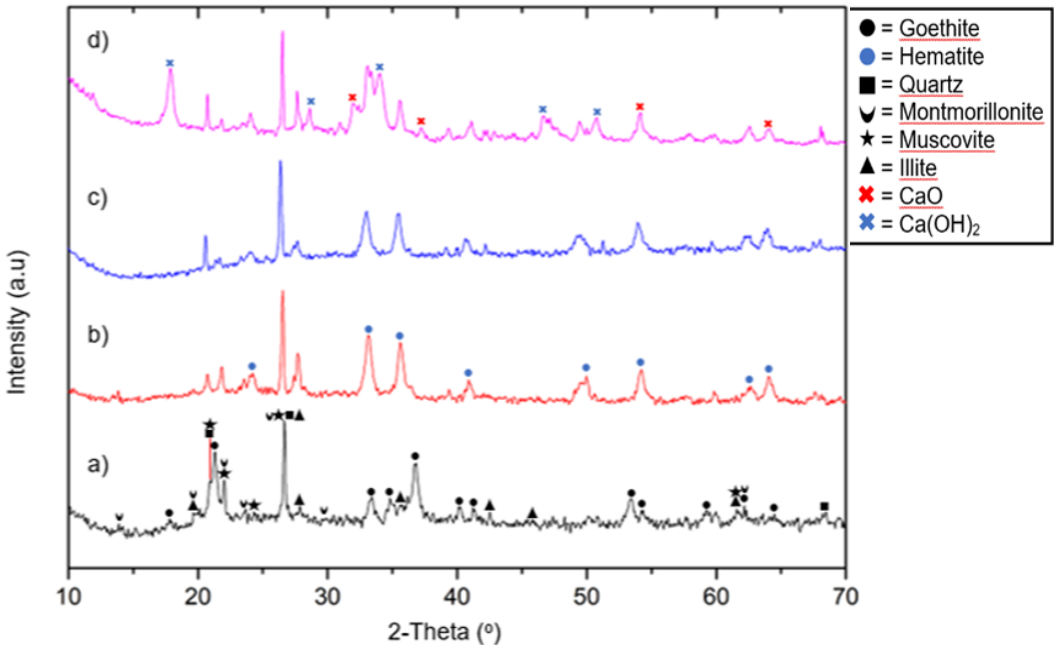

Figure 6. Difractogram of a) O-Clay, b) P-Clay, c) K-Clay, dan d) Ca-Clay.

Less P-Clay per volume of oil substrate was required to catalyze the transesterification compared to the other clays. The amount of catalytic activity is determined by the ability of the catalyst to convert methanol to methoxide [37]. An overview of the catalytic mechanism is showed in Figure 8.

3.6.2 Psychochemical properties of biodiesel product

GC-MS results indicate that the fatty acid methyl ester (FAME) produced in the transesterification reactions mediated by all catalyst combinations trialed (Table 3) had carbon chains 17-21 and were up to the biodiesel standard, 12-22 (Table 1). However, the variations in the areas of the GC-MS peaks showed that the FAME yield varied greatly with the 5% Ca-Clay catalyst producing the highest FAME yield. Table 4 shows that the range of viscosity values was up to ASTM D-445-10 standards at 1.9-6.0 mm^2/s. These values all exceed the minimum standard indicating the transesterification reactions were carried out at appropriate reaction temperatures and for sufficient reaction times [38,39].

Biodiesel density measurements were carried out using a pycnometer and compared with the ASTM standard range for biodiesel density of 0.86-0.90 g/cm^3. None of the biodiesel produced was within the ASTM standard. The biodiesel produced by the 5% Ca-Clay catalyst, however, was close to the ASTM standard. This is due to the presence of other large compounds, such as free fatty acids, glycerol, and fatty acids [38].

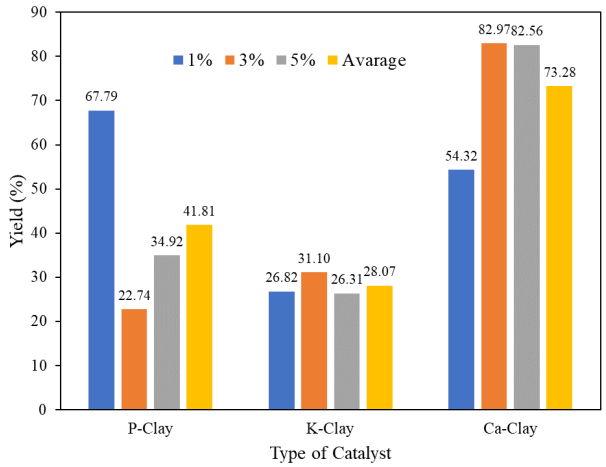

Figure 7. Biodiesel yield over various catalysts

4. Conclusions

Broiler chicken eggshells contained 70% calcium in the form of $CaCO_3$. Natural clay from Pasaman Barat contained 66.9% iron, 7.8%

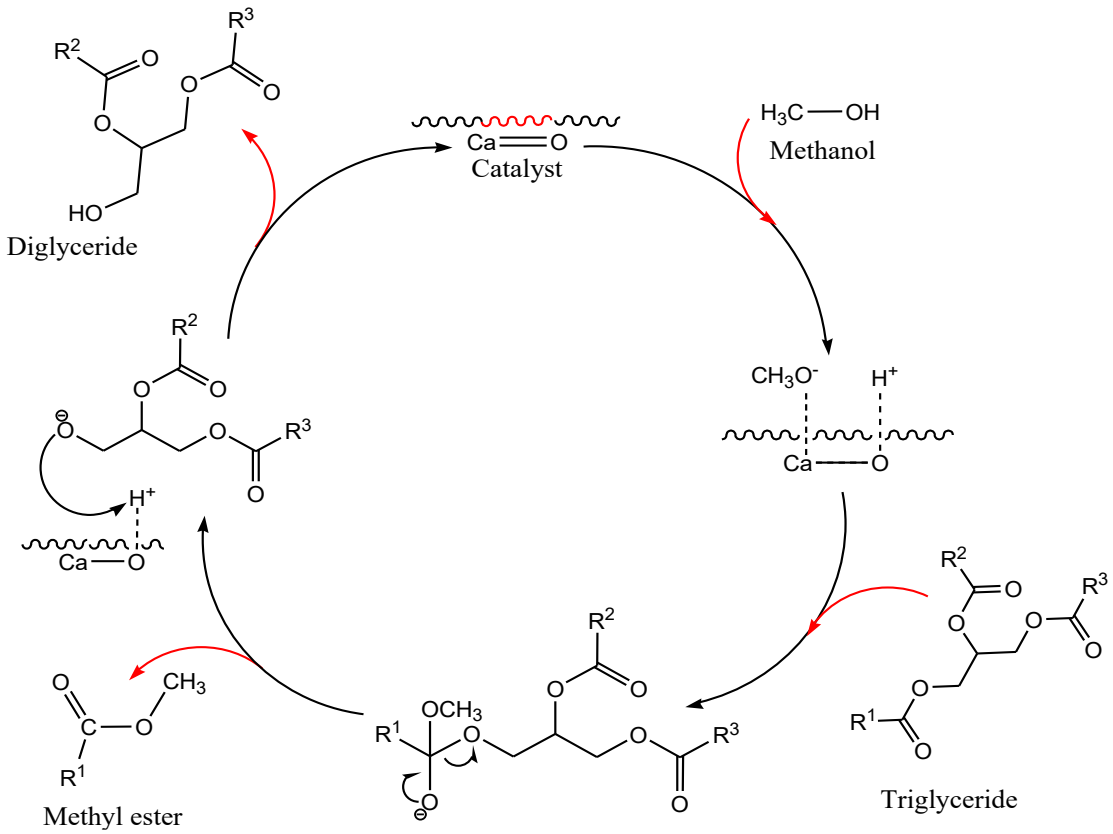

Figure 8. The catalytic cycle of CaO in the surface of the clay.

Table 3. GC-MS result of biodiesel product.

Catalyst Concentration	Retention Time	Compound Name	Molecule Formula	% Area
1% Catalyst P-Clay	16.015	Methyl palmitate	$C_{17}H_{34}O_2$	34.95
	17.830	Methyl elaidate	$C_{19}H_{36}O_2$	40.94
	18.043	Methyl stearate	$C_{19}H_{38}O_2$	3.75
3% Catalyst P-Clay	16.015	Methyl palmitate	$C_{17}H_{34}O_2$	27.91
	17.827	Methyl elaidate	$C_{19}H_{36}O_2$	36.42
	18.049	Methyl-15-Methyl Hexadecanoate	$C_{18}H_{36}O_2$	1.95
5% Catalyst P-Clay	16.015	Methyl palmitate	$C_{17}H_{34}O_2$	22.90
	17.822	Methyl elaidate	$C_{19}H_{36}O_2$	29.55
	18.039	Methyl stearate	$C_{19}H_{38}O_2$	2.23
1% Catalyst K-Clay	16.015	Methyl palmitate	$C_{17}H_{34}O_2$	12.96
	17.826	Methyl oleate	$C_{19}H_{36}O_2$	21.93
3% Catalyst K-Clay	16.013	Methyl palmitate	$C_{17}H_{34}O_2$	15.07
	17.819	Methyl Octadec-10-Enoate	$C_{19}H_{36}O_2$	20.56
5% Catalyst K-Clay	16.015	Methyl palmitate	$C_{17}H_{34}O_2$	15.48
	17.817	Methyl oleate	$C_{19}H_{36}O_2$	24.36
1% Catalyst Ca-Clay	16.020	Methyl palmitate	$C_{17}H_{34}O_2$	27.91
	17.833	Methyl oleate	$C_{19}H_{36}O_2$	31.91
3% Catalyst Ca-Clay	13.790	Methyl myristate	$C_{15}H_{30}O_2$	0.82
	16.026	Methyl palmitate	$C_{17}H_{34}O_2$	41.76
	17.839	Methyl elaidate	$C_{19}H_{36}O_2$	47.40
	18.049	Methyl stearate	$C_{19}H_{38}O_2$	4.35
5% Catalyst Ca-Clay	13.789	Methyl myristate	$C_{15}H_{30}O_2$	0.94
	16.034	Methyl palmitate	$C_{17}H_{34}O_2$	42.63
	17.846	Methyl elaidate	$C_{19}H_{36}O_2$	47.60
	18.048	Methyl stearate	$C_{19}H_{38}O_2$	4.37
	19.908	Arachidic acid methyl ester	$C_{21}H_{42}O_2$	0.38

Table 4. Biodiesel specification with catalyst variation.

Catalyst	Concentration (%)	Density (g/mL)	Viscosity @40 °C (mm^2/s)
P-Clay	1	0.93004	8.31
	3	0.93203	8.12
	5	0.93040	8.01
K-Clay	1	0.93087	9.69
	3	0.93343	8.89
	5	0.93504	8.44
Ca-Clay	1	0.93140	8.10
	3	0.93070	7.80
	5	0.93034	7.58
Biodiesel Standard		0.86-0.9 [38]	1.9–6.0 [39]

aluminum, and 20.5% silicon, with the dominant crystalline composition being goethite. Mixing and heating of CaO broiler chicken eggshells with natural clay of West Pasaman at 800 ^{o}C increased the calcium content of the clay to 57.8%. while decreasing iron (27.2%), aluminum (3.5%), and silicon (9.4%). Goethite crystals were changed into hematite, and $CaCO_3$ from the eggshells changed into CaO. Catalysts produced from heated clay, from KOH enhanced clay and CaO enhanced clay produced FAME chains of appropriate lengths for biodiesel. The catalytic activity of Ca-Clay performed better than P-Clay and K-Clay with a biodiesel yield of around 73%. On the other hand, smaller quantities of P-Clay were required to catalyze the oil substrate. As a result, the utilization of broiler chicken eggshell contributes to proper disposal of waste and provides a cheap catalyst in the transesterification reaction after purification to remove glycerol, and fatty acids so reducing the viscosity.

Acknowledgement

The authors would like to thank the LLPM of Andalas University for providing financial support in carrying out this work through research contract no. T/60/UN.16.17/PP.IS-KRP2GB/LPPM/2019.

References

[1] Canakci, M., Gerpen, J.V. (2007). Biodiesel production from jatropha oil with high free fatty acids. *Indian Journal of Natural Products and Resources*, 44(6), 1428−1436.

[2] Setiadji, S., Sundari, C.D.D., Munir, M., Fitriyah, S. (2018). Synthesis of solid catalyst from egg shell waste and clay for biodiesel production. *Journal of Physics: Conference Series*, 1013 (1), 1-6. DOI: 10.1088/1742-6596/1013/1/012199

[3] Yusuff, A.S., Adeniyi, O. D., Olutoye, M.A., Akpan, U.G. (2017). A Review on application of heterogeneous catalyst in the production of biodiesel from vegetable oils. *Journal of Applied Science & Process Engineering*, 4(2), 142–157. DOI: 10.1177/1077546316636361

[4] Meher, L.C., Vidya Sagar, D., Naik, S.N. (2006). Technical aspects of biodiesel production by transesterification - A review. *Renewable and Sustainable Energy Reviews*, 10(3), 248–268. DOI: 10.1016/j.rser.2004.09.002

[5] Huang, D., Zhou, H., Lin, L. (2011). Biodiesel: An alternative to conventional fuel. *Energy Procedia*, 16(PART C), 1874–1885. DOI: 10.1016/j.egypro.2012.01.287

[6] Zhou, C.H. (2011). An overview on strategies towards clay-based designer catalysts for green and sustainable catalysis. *Applied Clay Science*, 53(2), 87–96. DOI: 10.1016/j.clay.2011.04.016

[7] Wu, H., Zhang, J., Liu, Y., Zheng, J., Wei, Q. (2014). Biodiesel production from Jatropha oil using mesoporous molecular sieves supporting K_2SiO_3 as catalysts for transesterification. *Fuel Processing Technology*, 119, 114–120. DOI: 10.1016/j.fuproc.2013.10.021

[8] Fauzan, R., Syukri, S., Emdeniz, E. (2012). Optimasi aktifitas katalitik Co(II)- asetonitril yang diamobilisasi pada silika modifikasi dalam reaski transesterifikasi. *Journal Kimia Unand*, 1(1), 106–113.

[9] Sari F.N.N., Syukri, S., Zulhadjri, Z. (2013). Penentuan kondisi optimum aktivitas katalitik mangan(II) yang digrafting pada silika modifikasi. *Jurnal Kimia Unand*, *2*(1), 46–53.

[10] Akkari, M., Aranda, P., Ben Rhaiem, H., Ben Haj Amara, A., Ruiz-Hitzky, E. (2016). ZnO/clay nanoarchitectures: Synthesis, characterization and evaluation as photocatalysts. *Applied Clay Science*, 131, 131–139. DOI: 10.1016/j.clay.2015.12.013

[11] Ekeoma, M.O., Okoye, P. (2016). Anorthite clay formulation as catalyst for bio-diesel production. *J. Chem. Soc. Nigeria*, 41(2), 130–136.

[12] Abdelwahab Emam, E. (2019). Clay adsorption perspective on petroleum refining industry. *Industrial Engineering*, 2(1), 19−25. DOI: 10.11648/j.ie.20180201.13

[13] de Luna, M.D.G., Cuasay, J.L., Tolosa, N.C., Chung, T.W. (2017). Transesterification of soybean oil using a novel heterogeneous base catalyst: Synthesis and characterization of Na-pumice catalyst, optimization of transesterification conditions, studies on reaction kinetics and catalyst reusability. *Fuel*, 209, 246–253. DOI: 10.1016/j.fuel.2017.07.086

[14] Kwong, T.L., Yung, K.F. (2015). Heterogeneous alkaline earth metal-transition metal bimetallic catalysts for synthesis of biodiesel from low grade unrefined feedstock. *RSC Advances*, 5(102), 83748–83756. DOI: 10.1039/c5ra13819a

[15] Pandiangan, K.D., Jamarun, N., Arief, S., Simanjuntak, W., Rilyanti, M. (2016). The effect of calcination temperatures on the activity of CaO and CaO/SiO2 heterogeneous catalyst for transesterification of rubber seed oil in the presence of coconut oil as a co-reactant. *Oriental Journal of Chemistry*, 32(6), 3021–3026. DOI: 10.13005/ojc/320622

[16] Nurhayati, N., Muhdarina, M., Linggawati, A., Anita, S., Amri, T.A. (2015). Preparation

and characterization of calcium oxide heterogeneous catalyst derived from anadara granosa shell for biodiesel synthesis. *KnE Engineering*, 2016, 1–8. DOI: 10.18502/keg.v1i1.494

[17] Nuripati, N. (2019). Lempung Limau Manis: Modifikasi, karakterisasi, dan aktivitas katalitiknya. *Undergraduate Thesis*, Department of Chemistry, Universitas Andalas.

[18] Suryaputra, W., Winata, I., Indraswati, N., Ismadji, S. (2013). Waste capiz (Amusium cristatum) shell as a new heterogeneous catalyst for biodiesel production. *Renewable Energy*, 50, 795–799. DOI: 10.1016/j.renene.2012.08.060

[19] Buasri, A., Chaiyut, N., Loryuenyong, V., Wongweang, C., Khamsrisuk, S. (2015). Effect of eggshell as a filler on the mechanical properties of flexible polyurethane foam. *Sustainable Energy*, 1(2), 7–13. DOI: 10.12691/rse-1-2-1

[20] Thomas, R.E. (2010). High temperature processing of kaolinitic materials. *Doctoral Thesis*. School of Chemical Enginnering, The University of Birmingham.

[21] Aroke, U.O., Abdulkarim, A., Ogunbunka, R.O. (2013). Fourier-transform infrared characterization of kaolin, granite, bentonite and barite. *ATBU Journal of Environmental Technology*, 6(1), 42–53.

[22] Schroeder, P. (2002). Infrared spectroscopy in clay science. *CMS Workshop Lectures*, 11, 181-206.

[23] Rezende, J.C.T., Ramos, V.H.S., Oliveira, H.A., Oliveira, R.M.P.B., Jesus, E. (2018). Removal of Cr(VI) from aqueous solutions using clay from Calumbi geological formation, N. Sra. Socorro, SE State, Brazil. *Materials Science Forum*, 912, 1–6. DOI: 10.4028/www.scientific.net/msf.912.1

[24] Unuabonah, E.I., Günter, C., Weber, J., Lubahn, S., Taubert, A. (2013). Hybrid clay: A new highly efficient adsorbent for water treatment. *ACS Sustainable Chemistry and Engineering*, 1(8), 966–973. DOI: 10.1021/sc400051y

[25] Hongping, H., Ray, F.L., Jianxi, Z. (2004). Infrared study of HDTMA+ intercalated montmorillonite. *Spectrochimica Acta - Part A: Molecular and Biomolecular Spectroscopy*, 60(12), 2853–2859. DOI: 10.1016/j.saa.2003.09.028

[26] Qtaitat, M.A., Al-Trawneh, I.N. (2005). Characterization of kaolinite of the Baten El-Ghoul region/south Jordan by infrared spectroscopy. *Spectrochimica Acta - Part A: Molecular and Biomolecular Spectroscopy*, 61, 1519–1523. DOI: 10.1016/j.saa.2004.11.008

[27] Seprianti, S. (2017). Pemanfaatan tanah lempung alami (Clay) Limau Manis sebagai support katalis asam, karakterisasi dan aplikasi katalitiknya. *Undergraduate Thesis*, Department of Chemistry, Universitas Andalas.

[28] Mukasa-Tebandeke, I.Z., Ssebuwufu, P.J.M., Nyanzi, S.A., Schumann, A., Nyakairu, G.W.A., Ntale, M., Lugolobi, F. (2015). The Elemental, mineralogical, IR, DTA and XRD analyses characterized clays and clay minerals of central and Eastern Uganda. *Advances in Materials Physics and Chemistry*, 05(02), 67–86. DOI: 10.4236/ampc.2015.52010

[29] Tomic, Z., Antic-Mladenovic, S., Babic, B., Poharc-Logar, V., Djordjevic, A., Cupac, S. (2012). Modification of smectite structure by sulfuric acid and characteristics of the modified smectite. *Journal of Agricultural Sciences, Belgrade*, 56(1), 25–35. DOI: 10.2298/jas1101025t

[30] Louati, S., Baklouti, S., Samet, B. (2016). Geopolymers based on phosphoric acid and illito-kaolinitic clay. *Advances in Materials Science and Engineering*, 2016, 1–7. DOI: 10.1155/2016/2359759

[31] Beuntner, N., Thienel, C. (2015). Properties of calcined lias delta clay—technological effects, physical characteristics and reactivity in cement. *Calcined Clays for Sustainable Concrete*, 43-50. DOI: 10.1007/978-94-017-9939-3_6.

[32] Drzal, L.T., Rynd, J.P., Fort, T. (1983). Effects of calcination on the surface properties of kaolinite. *Journal of Colloid And Interface Science*, 93(1), 126–139. DOI: 10.1016/0021-9797(83)90392-2

[33] Hwidi, R.S., Izhar, T.N.T., Saad, F.N.M., Dahham, O.S., Noriman, N.Z., Shayfull, Z. (2018). Characterization of quicklime as raw material to hydrated lime: Effect of temperature on its characteristics. *AIP Conference Proceedings*, 2030, 020027-1-020027-7. DOI: 10.1063/1.5066668

[34] Longa-Avello, L., Pereyra-Zerpa, C., Casal-Ramos, J.A., Delvasto, P. (2017). Study of the calcination proces of two limonitic iron ores between 250 °C and 950 °C. *Revista Facultad de Ingeniería*, 26(45), 33–45. DOI: 10.19053/01211129.v26.n45.2017.6053

[35] Yusuff, A.S., Gbadamosi, A.O., Adeniyi, O.D., Olutoye, M.A., Akpan, U.G. (2018). A comparison of the effects of preparation variables on activity of composite anthill-chicken eggshell catalyst for biodiesel production. *Journal of Sustainability Science and Management*, 13(1), 133-146

[36] Soetaredjo, F.E., Ayucitra, A., Ismadji, S., Maukar, A.L. (2011). KOH/bentonite catalysts for transesterification of palm oil to biodiesel. *Applied Clay Science*, 53(2), 341–346. DOI: 10.1016/j.clay.2010.12.018

[37] Liu, X., He, H., Wang, Y., Zhu, S., Piao, X. (2008). Transesterification of soybean oil to biodiesel using CaO as a solid base catalyst. *Fuel*, 87(2), 216–221. DOI: 10.1016/j.fuel.2007.04.013

[38] Olutoye, M., Adeniyi, O.D., Yusuff, A.S. (2016). Synthesis of biodiesel from palm kernel oil using mixed clay-eggshell heterogeneous catalysts. *Iranica Journal of Energy and Environment*, 7(3), 308–314. DOI: 10.5829/idosi.ijee.2016.07.03.14

[39] Joshi, R.M., Pegg, M.J. (2007). Flow properties of biodiesel fuel blends at low temperatures. *Fuel*, 86(1–2), 143–151. DOI: 10.1016/j.fuel.2006.06.005